SHOCK-WAVE STRUCTURE ON HYPERSONIC FORWARD-FACING STEP FLOW

Paulo H. M. Leite, phmineiro@lcp.inpe.br
Wilson F. N. Santos, wilson@lcp.inpe.br
National Institute for Space Research, Combustion and Propulsion Laboratory, Cachoeira Paulista-SP, 12630-000 BRAZIL

Abstract. *Computations using the Direct Simulation Monte Carlo (DSMC) method are presented for hypersonic flow on forward-facing steps. The primary aim of this paper is to examine the step height impact on the shock-wave structure. The sensitivity of the shock-wave shape, shock-wave thickness and shock-wave layer to frontal-face height variations of such steps is investigated by using a model that classifies the molecules in three distinct classes: (1) undisturbed freestream, (2) reflected from the boundary and (3) scattered, i.e., molecules that had been indirectly affected by the presence of the step. The analysis showed that, for power-law shaped leading edge, the shock wave follows the body shape. It was found that the shock-wave layer for the forward-facing steps is in qualitative agreement with that for a flat plate without steps up to a certain distance from the step frontal face. After that, the shock-wave layer depends on the step frontal-face height.*

Keywords: *DSMC, Hypersonic Flow, Rarefield Flow, Forward-Facing Step, Shock-Wave.*

1. INTRODUCTION

Flow separation is a common phenomenon in aerodynamic configurations. This phenomenon usually occurs on any surface where the pressure rise and pressure gradient are sufficiently large. The importance of this phenomenon has been increased by the current interest in the calculation of the thermal and aerodynamic loads associated with imperfections or discontinuities, such as notches (Charwat, 1971; Howell and Korst, 1971), cavities (Charwat et al., 1961a,b; Everhart $et\ al.$, 2006; Everhart, 2009), gaps (Bertin and Goodrich, 1980; Hinderks $et\ al.$, 2004; Hinderks and Radespiel, 2006; Vharbonnier and Boerrigter, 1993), or steps (Grotowsky and Ballmann, 2000; Nestler et al., 1969; Pullin and Harvey, 1977; Wilkinson and East, 1968), that are often present on the surface of reentry space vehicles. For instance, the windward surface of the Space Shuttle entry configuration is thermally protected during the reentry trajectory by a system composed of a large number of tiles that are bonded to the vehicle aluminum structure. In order to account for thermal expansion between individual tiles, surface discontinuities like cavities, gaps or even steps, arising from the joints and possible title misalignment, are necessary between individual tiles. Such surface discontinuities may affect locally the flowfield structure and may cause higher than expected heating on the vehicle surface during the reentry trajectory.

For the particular case of steps, there is nowadays a rather extensive literature dealing with forward-facing step flows. In general, these research studies have been conducted in order to understand, among others, the physical aspects of a laminar or turbulent boundary layer in a subsonic (Camussi et al., 2008; Chapman et al., 1958; Stüer et al., 1999), supersonic (Bogdonoff and Kepler, 1955; Chapman et al., 1958; Driftmyer, 1973; Rogers and Berry, 1965; Uebelhack, 1969; Zukoski, 1967) or hypersonic (Grotowsky and Ballmann, 2000; Nestler et al., 1969; Pullin and Harvey, 1977; Wilkinson and East, 1968) flow past to this type of discontinuity, characterized by a sudden change on the surface slope. For the purpose of this introduction, it will be sufficient to describe only a few of these studies.

Rogers and Berry (1965) conducted an experimental investigation on forward-facing steps in a supersonic flow, $M \approx 2$, characterized by a thick laminar boundary layer. Freestream pressure was defined at 30, 50 and 70 μmHg, covering a Reynolds number per inch between 98 and 281. Eight step heights were tested, ranging in 0.1 inch intervals from 0.1 to 0.9 inches, except 0.8 inch. In addition, the step height was comparable with the local boundary-layer thickness for a flat-plate without steps. According to them, the investigation showed that the largest pressure rise occurred at the step face. In addition, it was found that this pressure rise depended on height-to-length (h/L) ratio, where h is the step height and L is the distance from the flat-plate leading edge to the step.

Forward-facing steps, for the particular case where the step heights h were less that the boundary-layer thickness δ, were investigated by Driftmyer (1973). The experimental investigation was conducted at a freestream Mach number of 4.9 with a unit Reynolds number in the range of 0.8-4.0$\times 10^6$ per foot. According to the experimental data, the pressure distributions measured in the separated region ahead of the steps were found to be functions of both Re_δ and h/δ for the turbulent boundary-layer separation case where $h < \delta$. It was also found that the pressure distribution on the step face was also a function of Re_δ and h/δ.

Pullin and Harvey (1977) numerically analyzed a two-dimensional rarefied hypersonic flow around a forward-facing step by considering N_2 as the working fluid, and freestream Mach number of 22. The analysis showed that in the vicinity of the step base, the flow has a rapid deceleration and compression accompanied by a sudden transition to a near continuum Navier-Stokes-type state nearly in equilibrium at the body temperature. In addition, their computational results presented good agreement with experimental data.

The major interest in these studies on forward-facing step available in the current literature has gone into considering

laminar or turbulent flow in the continuum flow regime. However, there is little understanding of the physical aspects of rarefied hypersonic flows past to steps related to the severe aerothermodynamic environment associated to a reentry vehicle. In this fashion, Leite and Santos (2009a) have studied forward-facing steps situated in a rarefied hypersonic flow by employing the DSMC method. The work was motivated by the interest in investigating the frontal-face height effect on the flowfield structure. A detailed and careful effort was made to provide a comprehensive description of the flow with special relevance to the particular case where the step height is less than the boundary-layer thickness. The primary emphasis was to examine the sensitivity of the velocity, density, pressure and temperature due to step-height variations of such forward-facing steps. The analysis showed that the hypersonic flow past a forward-facing step was characterized by a strong compression ahead of the frontal face. It was found that the recirculation region ahead of the steps was a function of the frontal-face height. The analysis also showed that disturbances upstream the step depended on changes in the frontal-face height of the steps. In addition, results showed that the separation point and the pre-separation region rely on the frontal-face height.

In continuation of the step research, Leite and Santos (2009b) extended the previous analysis (Leite and Santos, 2009a) by investigating the step-height effects on the aerodynamic surface quantities. In this manner, the investigation was undertaken in an attempt to assess the behavior of the heat transfer, pressure, and skin friction coefficients due to changes on the step height. The analysis found that locally high heating and pressure loads were observed on three locations along the step surface, i.e., on the lower surface, on the frontal face and on the upper surface. Results showed that both loads relied on the frontal-face height. The peak values for the heat transfer coefficient on the frontal-face surface were at least one order of magnitude larger than the maximum value observed for a smooth surface, i.e., a flat plate without a step.

In an effort to obtain further insight into the nature of the flowfield structure of forward-facing steps, under hypersonic transition flow conditions, the present account extends the previously analysis (Leite and Santos, 2009a,b) by examining computationally the shock-wave structure over the forward-facing steps. In the present study effort is directed to assess the behavior of the shock-wave shape, shock-wave thickness, and shock-wave layer on the steps. In pursuit of this goal, the Direct Simulation Monte Carlo (DSMC) method will be employed to investigate the shock-wave structure of the hypersonic two-dimensional flow over the steps.

2. STEP GEOMETRY DEFINITION

In the present work, discontinuities or imperfections on the surface of a reentry capsule is modeled by forward-facing steps. By considering that the step frontal-face h is much smaller than the nose radius R of a reentry capsule,i.e., $h/R \ll 1$, them, the hypersonic flow over the step may be considered as a hypersonic flow over a flat plate with a forward-facing step. Figure 1(a) displays a schematic view of the model employed and presents the important geometric parameters.

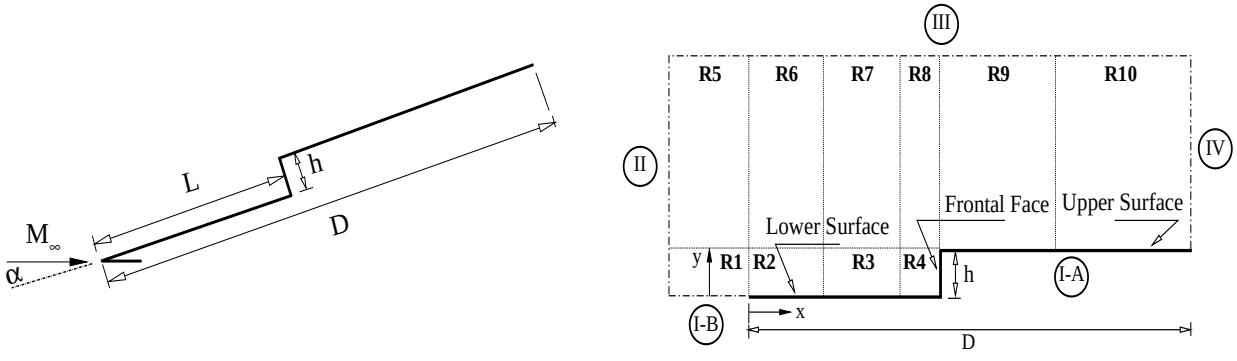

(a) Forward-facing step

(b) Computational domain

Figure 1. Drawing illustrating (a) the forward-facing step and (b) the computational domain.

Referring to Fig. 1(a), M_∞ represents the freestream Mach number, h the frontal-face height, D the total length of the forward-facing step, and L the location of the step. It was considered that the forward-facing step is infinitely long but only the length D is considered. It was assumed frontal-face height h of 3, 6 and 9 mm, which correspond to $H(= h/\lambda_\infty)$ of 3.23, 6.46, and 9.69, respectively, where λ_∞ is the freestream mean free path. In addition, it was also assumed L/λ_∞ of 50 and D/λ_∞ of 100.

An understanding of the frontal-face height impact on the flowfield structure can be gained by comparing the flowfield

behavior of a flat plate with a step to that of a plate without a step. In this fashion, a flat plate free of discontinuities, i.e, without steps, works as a benchmark for the cases with steps.

3. COMPUTATIONAL TOOL

The Direct Simulation Monte Carlo (DSMC) method, pioneered by Bird (1994), is a computational technique for modeling complex transitional flows of engineering interest. Is a particle simulation method that aims to calculate practical gas flows through computations of motions and collisions of modeled molecules. It has become one of the standard and reliable successful numerical techniques for rarefied gas flow simulations. In addition, it has been applied to many fields. These include the traditional field of rarefied atmospheric gas dynamics, the emerging field of micro-fluidics, and very-low pressure fields such as space propulsion and vacuum systems.

The DSMC method model a gas flow by using a computer to track the trajectory of simulated particles, where each simulated particle represents a fixed number of real gas particles. The particle evolution is divided into two independent phases during the simulation; the movement phase and the collision phase. In the movement phase, all particles are moved over appropriate distances related to a short time step, During this phase, some of the molecules interact with the domain boundaries. Molecules that strike the solid wall would reflect according to the appropriate gas-surface interaction model, specular, diffuse or a combination of both models. In the collision phase, intermolecular collisions are performed according to the theory of probability without time being consumed. In this manner, the intermolecular collisions are uncoupled to the translational molecular motion over the time step used to advance the simulation. The uncoupling of the molecular motion and collisions over small time steps and the division of the flowfield into small cells are the key computational assumptions associated with the DSMC method.

Collisions in the present DSMC code are simulated with the variable hard sphere (VHS) molecular model (Bird, 1981) and the no time counter (NTC) collision sampling technique (Bird, 1989). Energy exchange between kinetic and internal modes is controlled by the Borgnakke-Larsen statistical model (Borgnakke and Larsen, 1975). For the present account, the simulations are performed using a non-reacting gas model, consisting of 76.3% of N_2 and 23.7% of O_2, while considering energy exchange between translational, rotational and vibrational modes. For a given collision, the probability is defined by the inverse of the number of relaxation, which corresponds to the number of collisions needed, on average, for a molecule undergoes relaxation. The probability of an inelastic collision determines the rate at which energy is transferred between the translational and internal modes after an inelastic collision. Relaxation collision numbers of 5 and 50 were used for the calculations of rotation and vibration, respectively.

4. COMPUTATIONAL FLOW DOMAIN AND GRID

In order to implement the particle-particle collisions, the flowfield around the forward-facing step is divided into an arbitrary number of regions, which are subdivided into computational cells. The cells are further subdivided into subcells, two subcells/cell in each coordinate direction. The cell provides a convenient reference for the sampling of the macroscopic gas properties, while the collision partners are selected from the same subcell for the establishment of the collision rate. Therefore, the physical space network is used to facilitate the choice of molecules for collisions and for the sampling of the macroscopic flow properties such as density, velocity, pressure, temperature, etc.

The computational domain used for the calculation is made large enough so that body disturbances do not reach the upstream and side boundaries, where freestream conditions are specified. A schematic view of the computational domain is depicted in Fig. 1(b). According to this figure, side I-A is defined by the forward-facing step surface. Diffuse reflection with complete thermal accommodation is the condition applied to this side. In a diffuse reflection, the molecules are reflected equally in all directions, and the final velocity of the molecules is randomly assigned according to a half-range Maxwellian distribution determined by the wall temperature. Side I-B represents a plane of symmetry, where all flow gradients normal to the plane are zero. At the molecular level, this plane is equivalent to a specular reflecting boundary. Sides II and III are the freestream side through which simulated molecules enter and exit. Side II is positioned at $5\lambda_\infty$ upstream of the flat-plate leading edge, and side III defined at $30\lambda_\infty$, $34\lambda_\infty$, and $42\lambda_\infty$ above the step upper surface for frontal-face height H of 3.23, 6.46, and 9.69, respectively. Finally, the flow at the downstream outflow boundary, side IV, is predominantly supersonic and vacuum condition is specified (Bird, 1994). At this boundary, simulated molecules can only exit.

DSMC results depend on the cell size chosen, on the time step as well as on the number of particles per computational cell. In the DSMC code, the linear dimensions of the cells should be small in comparison with the length scale of the macroscopic flow gradients normal to the streamwise directions, which means that the cell dimensions should be the order of or smaller than the local mean free path (Alexander $et\ al.$, 1998, 2000). The time step should be chosen to be sufficiently small in comparison with the local mean collision time (Garcia and Wagner, 2000; Hadjiconstantinou, 2000). A very small time step results in an inefficient advancement of the solution and accumulation of statistics. Most particles will take many time steps to cross a given cell. As a result, the collision phase of each time step will involve the same group of particles as in the previous time step since almost no particles leave or enter the cell. Moreover, a large time step

Table 1. Region Dimensions ($x \times y$) and number of cells [$x \times y$] for cases H of 3.23, 6.46, and 9.69.

	H = 3.23	**H = 6.46**	**H = 9.69**
R1	$(5\lambda_\infty \times 3.23\lambda_\infty)[10 \times 10]$	$(5\lambda_\infty \times 6.46\lambda_\infty)[10 \times 20]$	$(5\lambda_\infty \times 9.69\lambda_\infty)[10 \times 30]$
R2	$(20\lambda_\infty \times 3.23\lambda_\infty)[40 \times 30]$	$(20\lambda_\infty \times 6.46\lambda_\infty)[40 \times 50]$	$(20\lambda_\infty \times 9.69\lambda_\infty][40 \times 60]$
R3	$(20\lambda_\infty \times 3.23\lambda_\infty)[40 \times 30]$	$(20\lambda_\infty \times 6.46\lambda_\infty)[40 \times 50]$	$(20\lambda_\infty \times 9.69\lambda_\infty)[60 \times 60]$
R4	$(10\lambda_\infty \times 3.23\lambda_\infty)[60 \times 70]$	$(10\lambda_\infty \times 6.46\lambda_\infty)[110 \times 120]$	$(10\lambda_\infty \times 9.69\lambda_\infty)[120 \times 140]$
R5	$(5\lambda_\infty \times 30\lambda_\infty)[10 \times 40]$	$(5\lambda_\infty \times 34\lambda_\infty)[10 \times 50]$	$(5\lambda_\infty \times 42\lambda_\infty)[10 \times 60]$
R6	$(20\lambda_\infty \times 30\lambda_\infty)[30 \times 40]$	$(20\lambda_\infty \times 34\lambda_\infty)[30 \times 50]$	$(20\lambda_\infty \times 42\lambda_\infty)[30 \times 60]$
R7	$(20\lambda_\infty \times 30\lambda_\infty)[30 \times 40]$	$(20\lambda_\infty \times 34\lambda_\infty)[30 \times 50]$	$(20\lambda_\infty \times 42\lambda_\infty)[30 \times 60]$
R8	$(10\lambda_\infty \times 30\lambda_\infty)[30 \times 50]$	$(10\lambda_\infty \times 34\lambda_\infty)[30 \times 60]$	$(10\lambda_\infty \times 42\lambda_\infty)[30 \times 80]$
R9	$(25\lambda_\infty \times 30\lambda_\infty)[60 \times 70]$	$(25\lambda_\infty \times 34\lambda_\infty)[70 \times 90]$	$(25\lambda_\infty \times 42\lambda_\infty)[70 \times 90]$
R10	$(25\lambda_\infty \times 30\lambda_\infty)[60 \times 80]$	$(25\lambda_\infty \times 34\lambda_\infty)[60 \times 80]$	$(25\lambda_\infty \times 42\lambda_\infty)[70 \times 80]$

allows the molecules to move too far without the opportunity to participate in a collision. This again causes a smearing of the properties of the flow, resulting in non-physical results. Therefore, the time step must be chosen such that a typical particle moves about one fourth of the cell dimension at each time step. Finally, the number of simulated particles has to be large enough to make statistical correlations between particles insignificant.

As part of the verification process, a grid independence study was made with three different structured meshes, coarse, standard and fine, in each coordinate direction. The effect of altering the cell size in the x- and y-directions was investigated for a coarse and fine grids with, respectively, 50% less and 100% more cells with respect to the standard grid. Table 1 summarizes the main characteristics for the standard grid related to ten regions (R1 to R10 in Fig. 1(b)) for the frontal-face height H of 3.23, 6.46, and 9.69. In this fashion, for H of 3.23, 6.46, and 9.69, the total number of cells correspond, respectively, to 20,000, 33,800, and 41,600 cells.

A discussion of the verification process, effects of cell size and number of molecules on the aerodynamic surface quantities for the forward-facing steps presented herein, is described in detail in Leite (2009). Furthermore, as part of the validation process, results for density, velocity and translational temperature were compared with those obtained from other established DSMC code and experimental data in order to ascertain how well the DSMC code employed in this study is able to predict hypersonic flow in a flat plate. Details of this comparison is also presented in Leite (2009).

5. FREESTREAM AND FLOW CONDITIONS

Freestream conditions and gas properties employed in the present calculations are those given by Leite (2009) and tabulated in Tabs. 2 and 3, respectively. These flow conditions represent those experienced by a Brazilian capsule, named SARA (acronyms for SAtélite de Reentrada Atmosférica) at an altitude of 70 km.

Table 2. Freestream flow conditions

Altitude (km)	T_∞(K)	p_∞(N/m^2)	ρ_∞(kg/m^3)	μ_∞(Ns/m^2)	n_∞(m^{-3})	λ_∞(m)
70	219.69	5.582	8.753×10^{-5}	1.455×10^{-5}	1.8192×10^{21}	9.285×10^{-4}

Referring to Tabs. 2 and 3, T_∞, p_∞, ρ_∞, μ_∞, n_∞, λ_∞, and U_∞ stand respectively for temperature, pressure, density, viscosity, number density, and mean free path, and X, m, d, and ω account respectively for mole fraction, molecular mass, molecular diameter and viscosity index.

Table 3. Gas properties

	X	m (kg)	d (m)	ω
O_2	0.237	5.312×10^{-26}	4.01×10^{-10}	0.77
N_2	0.763	4.650×10^{-26}	4.11×10^{-10}	0.74

The freestream velocity U_∞, assumed to be constant at 7456 m/s, corresponds to a freestream Mach number M_∞ of 25. This is the Mach number for SARA capsule at 70 km of altitude. The wall temperature T_w is assumed constant at 880 K. This temperature is chosen to be representative of the surface temperature near the stagnation point of the SARA reentry capsule and is assumed to be uniform in the entire surface of the forward-facing step. It is important to mention that the surface temperature is low compared to the stagnation temperature of the air. This assumption seems to be reasonable since practical surface materials will

probably be destroyed if surface temperature is allowed to approach the stagnation temperature.

By assuming the frontal-face height h as the characteristic length, the Knudsen number Kn_h corresponds to 0.3095, 0.1548 and 0.1032 for height h of 3, 6 and 9 mm, respectively. The Reynolds number Re_h is around 136, 272 and 409 for height h of 3, 6 and 9 mm, respectively, also based on the frontal-face height h and on conditions in the undisturbed stream. Finally, it was assumed zero-degree angle of attack, i.e., $\alpha = 0$.

6. COMPUTATIONAL PROCEDURE

The problem of predicting detachment, thickness and shape of shock waves has been stimulated by the necessity for blunt noses and leading edges configurations designed for hypersonic flight in order to cope with the aerodynamic heating. In addition, the ability to predict thickness, shape and location of shock waves is of primary importance in analysis of aerodynamic interference. Furthermore, the knowledge of the shock-wave displacement is also especially important in waverider configurations, since these hypersonic configurations usually rely on shock-wave attachment at the leading edge to achieve their high lift-to-drag ratio at high-lift coefficient.

In the present account, the shock-wave structure, defined by shock shape (location), shock thickness, and shock layer, is predicted by employing a procedure based on the physics of the particles (Santos, 2008). In this procedure, the flow is assumed to consist of three distinct classes of molecules: Class I molecules denote those molecules from the freestream that have not been affected by the presence of the body surface; Class II molecules are those molecules that have struck and been reflected from the body surface at some time in their past history; and finally, those molecules that have been indirectly affected by the presence of the body are defined as class III molecules. Figure 2(a) illustrates schematically the definition for the molecular classes.

Moreover, it is assumed that the class I molecule changes to class III molecule when it collides with either class II or class III molecule. Class I or class III molecule is progressively transformed into class II molecule when it interacts with the body surface. Also, a class II molecule remains class II independently of subsequent collisions and interactions. Hence, the transition from class I molecules to class III molecules may represent the shock wave, and the transition from class III to class II may define the boundary layer on the body surface.

A typical distribution of class III molecules perpendicular to the flat-plate surface is displayed in Fig. 2(b) along with the definition used to determine the thickness, layer and center of the shock wave. In this figure, Y is the height y normal to the flat-plate surface, normalized by the freestream mean free path λ_∞, and f_{III} is the ratio of the number of molecules for class III inside the cell to the total number of molecules inside the same cell.

In a rarefied flow, the shock wave has a finite region that depends on the transport properties of the gas, and can no longer be considered as a discontinuity obeying the classical Rankine-Hugoniot relations. In this fashion, the shock layer is defined as being the distance between the shock wave center and the flat-plate surface, as shown in Fig. 2(b). Still referring to Fig. 2(b), the center of the shock wave is defined by the station that corresponds to the maximum value for f_{III}. Forthermore, the shock-wave thickness δ is defined by the distance between the stations that correspond to the mean value for f_{III}. Finally, the shock-wave shape or "shock-wave location" is determined by the coordinate points given by

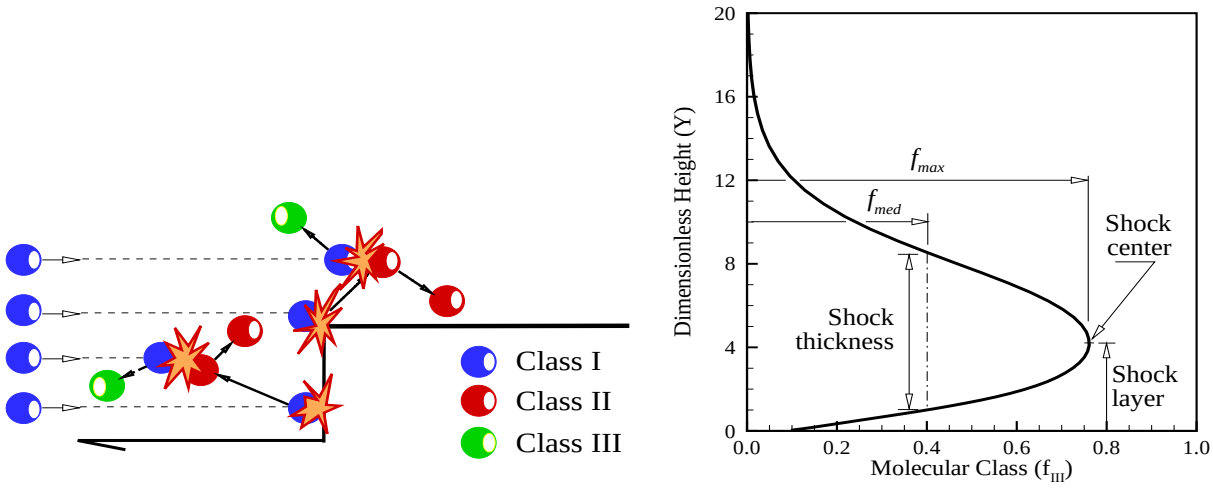

(a) Molecular class

(b) Shock-wave structure

Figure 2. Drawing illustrating (a) the classification of molecules, and (b) the shock-wave structure.

the maximum value in the f_{III} distribution along the flat-plate surface, i.e., y-direction as shown in Fig. 1(b).

7. COMPUTATIONAL RESULTS AND DISCUSSION

This section focuses on the effects that take place on the shock-wave structure due to variations on the step frontal-face height. In this scenario, the purpose of this section is to discuss and to compare differences in the thickness, location, and shape of the shock wave due to variations on the frontal-face height h. Nevertheless, having computed molecular class properties over the entire computational domain, it proves instructive to summarize first the major features of the results related to the class of molecules.

7.1 Molecular Class Distribution

The distribution of molecules for classes I, II, and III is demonstrated in Fig. 3 for three sections along the step lower surface. In this set of plots, f_I, f_{II} and f_{III} are the ratio of the number of molecules for class I, II and III, respectively, to the total amount of molecules inside each cell along the y-direction, X and Y are the length x and height y along the step surface normalized by the freestream mean free path λ_∞. Also, filled and empty symbols correspond to molecular class distribution for dimensionless height H of 3.23 and 9.69, respectively. The distribution for the H = 6.46 case is intermediate to these cases, and it will no be shown. For comparison purpose, the molecular class distribution for the flat-plate case, i.e, a flat plate without steps, is also presented in this set of plots. In this manner, for the flat-plate case, classes I, II, and III correspond to the solid, dash, and dashdot lines, respectively. It should be remarked that the steps are positioned at section X = 50.

According to Fig. 3, it can be observed that, for section X = 28, the molecular class profiles for the steps are identical, by visual inspection, to those for the flat-plate case. It means that no effects due to the presence of the steps are observed up to this section. However, for sections $X \geq 38$, the upstream disturbance caused by the steps is observed on the molecular class profiles. In addition, it is recognized that the downstream evolution of the flow along the lower surface displays a smearing tendency of the shock wave, formed at the leading edge of the lower surface, due to the displacement of the maximum value for the molecular class III distribution, as defined in the shock-wave structure shown in Fig.2(b). Moreover, the region defined by class II molecules is related to the boundary layer on the step surface. In this respect, it is clearly seen that the boundary layer for the H = 9.69 case is larger than that for the H = 3.23 case close to the frontal face of the steps. This is an expected behavior since the "body" defined by the step with H = 3.23 is more "streamlined" than that for H = 9.69 case.

Of great significance in this set of plots is the behavior of the molecules at the vicinity of the lower surface. It should be noticed that molecules from freestream, represented by class I molecules, basically do not penetrate into the boundary layer and do not reach the surface for the H = 9.69 case at section X = 48, as shown in Fig. 3(c). In contrast, molecules from freestream penetrate into the boundary layer and a small amount collides with the lower surface for the other cases at sections $X < 48$, even after the establishment of the steady state. This situation is illustrated in Fig. 3(a,b). An understanding of this behavior can be gained by the distribution of density at the vicinity of the lower surface. Figure 4 displays the density ratio ρ/ρ_∞ profiles for the same three sections. It is apparent from this set of plots that density ratio

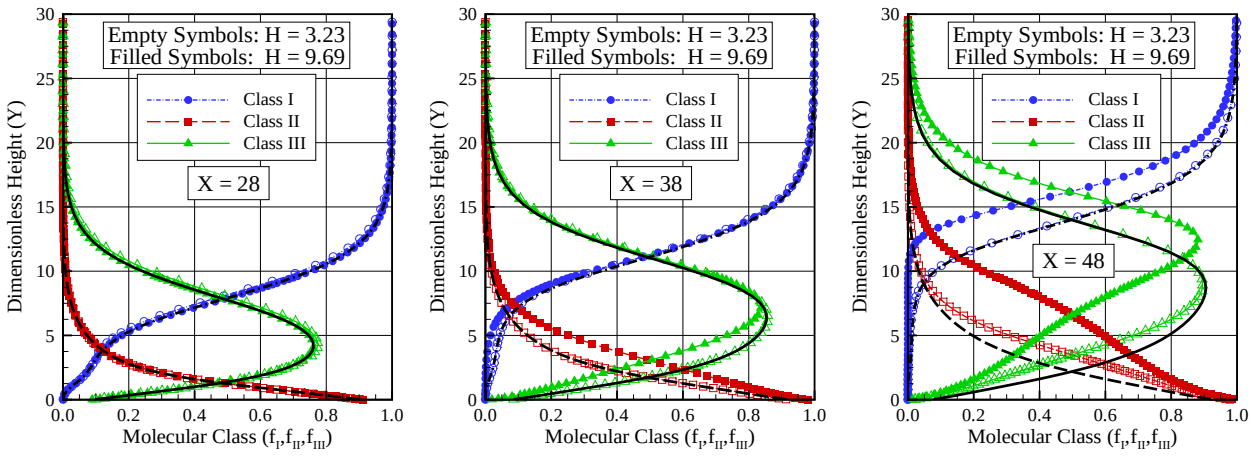

Figure 3. Distribution of molecules for classes I, II and III for three sections along the lower surface of the forward-facing step as a function of the dimensionless height H.

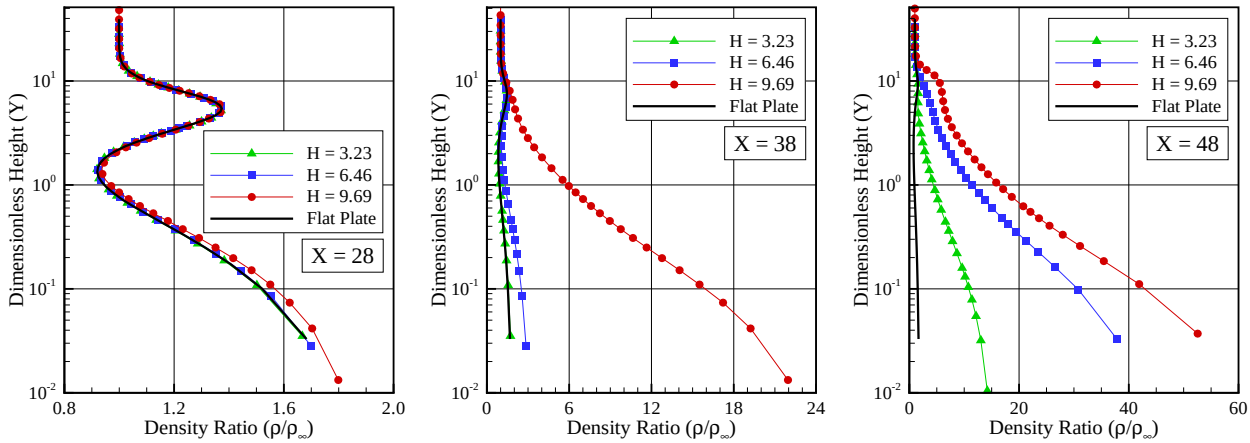

Figure 4. Distribution of density ratio (ρ/ρ_∞) profile along the lower surface of the forward-facing step as a function of the dimensionless frontal-face height H

increases significantly with increasing the step height H and reaches its maximum value at the stagnation point, at the base of the steps. In this fashion, the buildup of particle density near the frontal face acts as a shield for the molecules coming from the undisturbed stream, which are represented by class I molecules. This density rise at the vicinity of the frontal face is a characteristic observed in blunt-body reentry flow, known as a cold-wall flow. Usually, in a reentry flow, the wall temperature T_w is low compared to the stagnation temperature T_o. For this particular investigation, this ratio is 0.032.

The distribution of molecules for classes I, II and III for three sections along the upper surface of the steps is displayed in Fig. 5. In this group of plots, Y' is the distance $(y-h)$ above the upper surface of the steps normalized by the mean free path λ_∞. Again, filled and empty symbols correspond to the molecular class distribution for step height H of 3.23 and 9.69, respectively. It is clearly seen in this group of plots that the distribution of molecules for classes I, II and III presents a similar behavior as that observed for the step lower surface in the sense that the shock-wave layer and shock-wave thickness continue to increase as the flow develops along the upper surface of the steps.

Before proceeding with the shock-wave structure analysis, it is desirable to present the distribution of the molecular classes around the forward-facing steps. In this way, particular attention is paid to the molecular class III for the forward-facing steps investigated. Figure 6 exhibits the contour map for class III molecules with streamline traces. In this group of diagrams, X and Y correspond to the length x and height y normalized by the freestream mean free path λ_∞. It is important to mention that class III molecules represent the effect of the presence of the step that is propagated in the off-body direction. According to this set of diagrams, the disturbance in the off-body direction is more significant for the

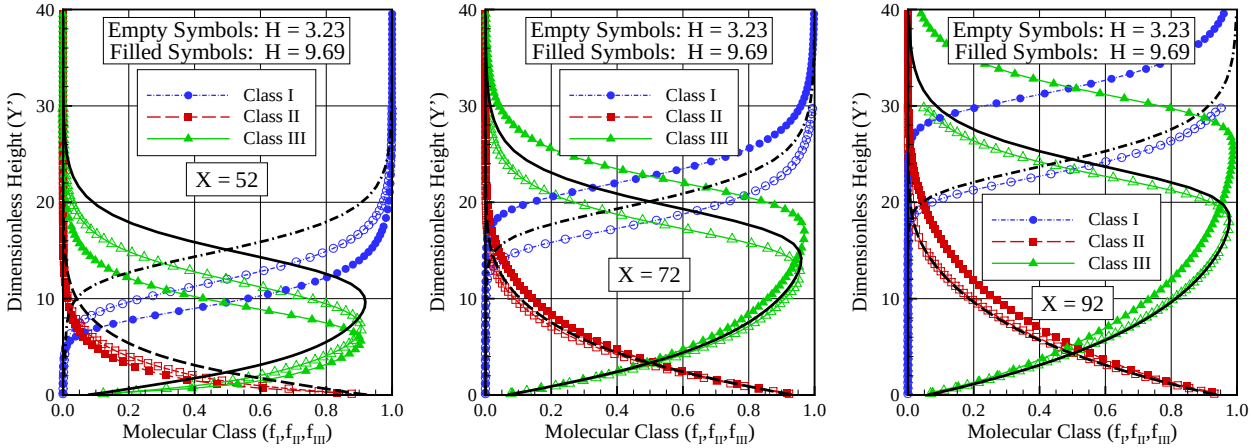

Figure 5. Distribution of molecules for classes I, II and III for three sections along the upper surface of the forward-facing step as a function of the dimensionless height H.

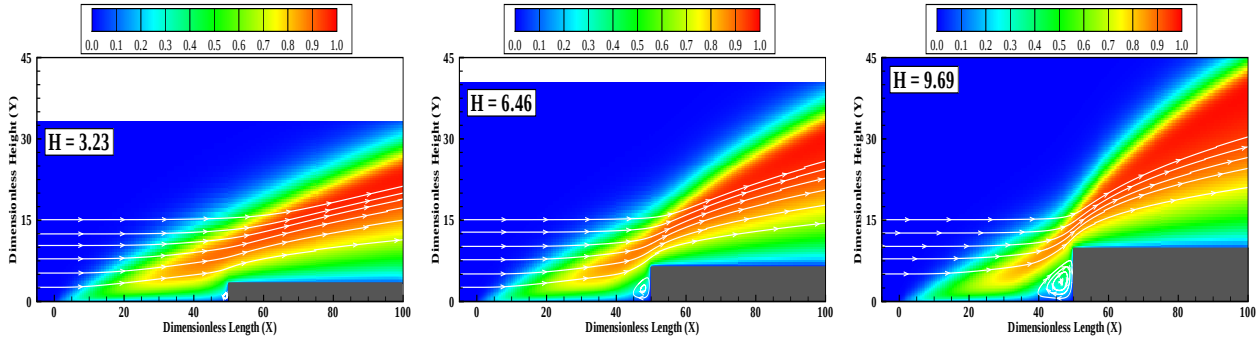

Figure 6. Contour map with streamline traces for class III molecules around the forward-facing step with dimensionless height H of 3.23 (left), 6.46 (middle) and 9.69 (right).

H = 9.69 case than that for the H = 3.23 case, as would be expected.

7.2 Shock-Wave Shape

The shock-wave shape, defined by the shock-wave center, is obtained by calculating the position that corresponds to the maximum f_{III} in the y-direction along the step surface, as defined by Fig. 2(b). Figure 7 displays the shock-wave shape as a function of the dimensionless frontal-face height H. As a base of comparison, the shock-wave shape for the flat-plate case is also displayed in the same figure.

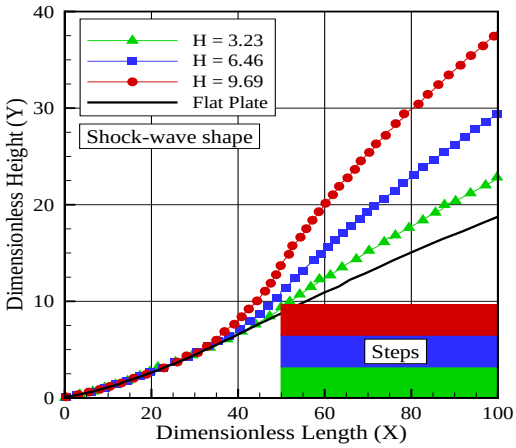

Figure 7. Shock-wave shape over the forward-facing step as a function of the dimensionless frontal-face height H.

8. CONCLUDING REMARKS

This study applies the Direct Simulation Monte Carlo (DSMC) method to assess the effect on the shock-wave structure due to variations on the face height of forward-facing steps. The calculations provided information concerning the nature of the shock-wave shape, shock-wave thickness, and shock-wave layer resulting from variations on the frontal face for the idealized situation of two-dimensional hypersonic rarefied flow.

The computational results indicated that the shock-wave layer for the steps grows similar to the for the flat-plate case, i.e., a flat plate without steps, up to a certain distance from the step frontal face. After that, the shock-wave layer for the step continues to increase as a function of the frontal-face height. In addition, a similar behavior was found for the shock-wave shape.

9. ACKNOWLEDGEMENTS

The authors would like to thank the financial support provided by CNPq (Conselho Nacional de Desenvolvimento Científico e Tecnológico) under Grant No. 473267/2008-0.

10. REFERENCES

Alexander, F. J., Garcia, A. L., and Alder, B. J., 1998. "Cell Size Dependence of Transport Coefficient in Stochastic Particle Algorithms", Physics of Fluids, Vol. 10, pp. 1540–1542.

Alexander, F. J., Garcia, A. L., and Alder, B. J., 2000. "Erratum: Cell Size Dependence of Transport Coefficient in Stochastic Particle Algorithms", Physics of Fluids, Vol. 12, pp. 731–731.

Bertin, J. J., and Goodrich, W. D., 1980. "Aerodynamic Heating for Gaps in Laminar and Trasitional Boundary Layers", 18th AIAA Aerospace Sciences Meeting and Exhibit, AIAA Paper 80–0287, Pasadena, CA, USA, January 14–16,.

Bird, G. A., 1981. "Monte Carlo Simulation in an Engineering Context", In Fisher, S. S., ed., Progress in Astronautics and Aeronautics: Rarefied gas Dynamics, Vol. 74, part I, AIAA New York, pp. 239–255.

Bird, G. A., 1989. "Perception of Numerical Method in Rarefied Gasdynamics", In Muntz, E. P., Weaver, D. P., and Capbell, D. H., eds., Rarefied Gas Dynamics: Theoretical and Computational Techniques, Vol. 118, Progress in Astronautics and Aeronautics, AIAA, New York, pp. 374–395.

Bird, G. A., 1994. Molecular Gas Dynamics and the Direct Simulation of Gas Flows, Oxford University Press.

Bogdonoff, S. M. and Kepler, C. E., 1955. "Separation of a supersonic turbulent boundary layer", Journal of The Aeronautical Science, VOl. 22, pp. 414–430.

Borgnakke, C. and Larsen, P. S., 1975. "Statistical Collision Model for Monte Carlo Simulation of Polyatomic Gas Mixture", Journal of Computational Physics, Vol. 18, No. 4, pp. 405–420.

Camussi, R., Felli, M., Pereira, F., Aloisio, G., and DiMarco, A., 2008. "Statistical properties of wall pressure fluctuations over a forward-facing step", Physics of Fluids, Vol. 20, pp. 075113.

Chapman, D. R., Kuehn, D. M., and Larson, H. K., 1958. "Investigation of separeted flows in supersonic and subsonic streams with emphasis on the effect of transition", NACA Report 1356.

Charwat, A. F., Roos, J. N., Dewey Jr., C. F., & Hitz, J. A., 1961a. "An investigation of separated flows – Part I: The pressure field", Journal of Aerospace Sciences, Vol. 28, pp. 457–470.

Charwat, A. F., Dewey Jr., C. F., Roos, J. N. & Hitz, J. A., 1961b. "An investigation of separated flows – Part II: Flow in the cavity and heat transfer", Journal of Aerospace Sciences,Vol. 28, pp. 513–527.

Charwat, A. F., 1971. "Separation of a supersonic accelerated flow over notches", AIAA Journal,Vol. 9, pp. 1656–1657.

Driftmyer, R. T., 1973. "A forward facing step study: the step height less than the boundary-layer thickness", NOLTR 73-98, Naval Ordinance Laboratory, White Oak, Maryland.

Everhart, J. L., Alter, S. J., Merski, N. R., and Wood, W. A., and Prabhu, R. K., 2006. "Pressure Gradient Effects on Hypersonic Cavity Flow Heating", 44th AIAA Aerospace Sciences Meeting and Exhibit, AIAA Paper 2006–0185, Reno, NV.

Everhart, J. L., 2009. "Supersonic/hypersonic laminar heating correlations for rectangular and impact-induced open and closed cavities", Journal of Spacecraft and Rockets, Vol. 46, pp. 545–560.

Garcia, A. L., and Wagner, W., 2000. "Time Step Truncation Error in Direct Simulation Monte Carlo", Physics of Fluids, Vol. 12, pp. 2621–2633.

Grotowsky, M. G., and Ballmann J., 2000. "Numerical investigation of hypersonic step-flows", Shock Waves, Vol. 10, pp. 57–72.

Hadjiconstantinou, N. G., 2000. "Analysis of Discretization in the Direct Simulation Monte Carlo", Physics of Fluids, Vol. 12, pp. 2634–2638.

Hinderks, M., Radespiel, R., and Gülhan, A., 2004. "Simulation of Hypersonic Gap Flow with Consideration of Fluid Structure Interaction", 34th AIAA Fluid Dynamics Conference and Exhibit, AIAA Paper 2004–2238, Portland, OR.

Hinderks, M. and Radespiel, R., 2006. "Investigation of Hypersonic Gap Flow of a Reentry Nosecap with Consideration of Fluid structure Interaction", 44th AIAA Aerospace Sciences Meeting and Exhibit, AIAA Paper 2006-0188, Reno, NV, USA, January 9–12, 2006.

Howell, R. H., and Korst, H. H., 1971. "Separation controlled transonic drag-Rise modification for V-shaped notches", AIAA Journal, Vol. 9, pp. 2051–2057.

Leite, P. H. M., and Santos, W. F. N., 2009a. "Direct Simulation of Low Density Hypersonic Flow over a Foward-Facing Step". 20th International Congress of Mechanical Engineering, COBEM 2009, November 15–20, Gramado, RS, Brazil.

Leite, P. H. M., and Santos, W. F. N., 2009b. "Numerical Investigation of Heat Transfer and Pressure Distribution of Hypersonic Flow over a Forward-Facing Step". 30th Iberian-Latin-American Congress on Computational Methods in Engineering, CILAMCE 2009, November 5–8, Armação de Búzios, RJ, Brazil.

Leite, P. H. M., 2009. Direct simulation of the step influence on a reentry vehicle Surface (in Portuguese). *MS Thesis*, INPE (National Institute for Space Research), Brazil.

Nestler, D. E., Saydah, A. R., and Auxer, W. L., 1969. "Heat transfer to steps and cavities in hypersonic turbulent flow", AIAA Journal, Vol. 7, pp. 1368–1370.

Pullin, D. I., and Harvey, J. K., 1977. "Direct simulation calculations of the rarefied flow past a forward-facing step", AIAA Journal, Vol. 15, pp. 124–126.
Rogers, E. W. E., and Berry, C. J., 1965. "Research at the NPL on the influence at supersonic speeds and low Reynolds numbers of thick laminar boundary layers", Advances in Applied Mechanics: Rarefied Gas Dynamics (ed. J. H. Leeuw, J. H.), Vol I, Suppl. 3, pp. 574–591, Academic Press, New York.
Santos, W. F. N., 2008. "Physical and computational aspects of shock waves over power-law leading edges", Physics of Fluids, Vol. 20, pp. 016101.
Stüer, H., Gyr, A., and Kinzelbach, W., 1999. "Laminar separation on a forward facing step", Eur. J. Mech. B/Fluids, Vol. 18, pp. 675–6920.
Wilkinson, P. R. and East, R. A., 1968. "Mean properties of a region of separation in laminar hypersonic flow", AIAA Journal, Vol. 6, pp. 2183–2184.
Uebelhack, H. T., 1969. "Turbulent flow separation ahead of forward facing steps in supersonic two-dimensional and axisymmetric flows", Report VKI-TN-54, Von Karman Institute for Fluid Dynamics.
Vharbonnier, J., and Boerrigter, H., 1993. "Contribution to the Study of Gap Induced Boundary Layer Transition in Hypersonic Flow", AIAA/DGLR 5th International Aerospace Planes and Hypersonics Technologies Conference, AIAA Paper 93–5111, Munich, Germany.
Zukoski, E. E., 1967. "Turbulent boundary-layer separation in front of a forward-facing step", AIAA Journal, Vol. 5, pp. 1746–1753.

11. Responsibility notice

The authors are the only responsible for the printed material included in this paper.